

Position and Orientation Determination For a Guided K-9

Jeff Miller, *Auburn University*
David M. Bevly, *Auburn University*

BIOGRAPHY

Jeff Miller is pursuing his PhD in Mechanical Engineering (M.E.) at Auburn University. He graduated from the University of Texas at Arlington with a B.S. in M.E. in 2005 and an M.S. in M.E. in 2006. He also earned a B.S. in Physical Science from Freed-Hardeman University. He works in the GPS and Vehicle Dynamics Laboratory studying the navigation and control of canines.

David M. Bevly is an assistant professor at Auburn University and head of the GPS and Vehicle Dynamics Laboratory. He received his Ph.D in Mechanical Engineering from Stanford University in 2001, his M.S. in M.E. from Massachusetts Institute of Technology in 1997, and his B.S. in M.E. from Texas A&M University in 1995.

ABSTRACT

A GPS/INS sensor suite was attached by a vest to a canine (K-9) in order to attain characteristic position and orientation data during typical K-9 behavioral motions such as walking, trotting, sitting, and turning. For better accuracy, the sensors were combined using an Extended Kalman Filter (EKF), which has been done for other GPS/INS integrated systems [1-3] and then examined to see if the position and orientation EKF outputs correctly portrayed the K-9 motions. Special tuning of the EKF was required due to the unique motion characteristics inherent in canines. However, the EKF was found to be effective in achieving relatively accurate position and orientation tracking results for the canine. Results show that the low-cost GPS/INS system can provide information about the canine's motion, including the canine's current position and heading.

INTRODUCTION

The use of GPS and INS integration to accurately localize vehicles and robots for remote or autonomous control purposes is very prevalent today [2-6]. However, little

work has been done on remote or autonomous control of live systems (bio-robots), such as canines. GPS/INS integration has been effectively utilized in tracking the motion of pedestrians and horses [7-9]. Reports of the successful implantation or coming research involving the implantation of electrodes in the brains of animals such as sharks, rats, monkeys, spiny dogfish, mice, pigeons, and even cockroaches for controlling purposes are available to date [10-17]. The ability to autonomously control a dog could have an immediate impact in search and rescue missions, narcotic detection, or bomb detection, and ultimately, could save human lives since the handler can be invisible and/or out of harm's way. Also, dogs can traverse a variety of terrain more efficiently than humans, and possess a natural array of "sensors" used to detect and locate items of interest. Therefore, many aspects that pose problems to Unmanned Ground Vehicles (UGVs) are inherently removed with the canine, as the dog can execute the low-level decision making necessary for rerouting its local path to avoid obstacles or unfavorable terrain. Also, since these canines are trained to scour an entire area when they reach the general destination that a handler guides them to, a relatively small amount of error in estimating the dog's position and orientation may be acceptable.

Auburn University's Canine & Detection Research Institute (CDRI) has trained canines to move to desired locations by responding to different tones, rather than by utilizing brain electrodes. A command module produces tones to provide instruction. A reinforcing tone (static) is given to the K-9 to communicate that it is traveling in the right direction. When the tone is stopped, the K-9 turns in different directions until it is positioned accurately. Then, the reinforcing tone is re-established, and the K-9 continues going straight. It has been established that a K-9 can be remotely controlled in this fashion. The CDRI is currently working on broadening the array of available commands to include gentle vibrations that will tell the dog to turn left or right.

The long-term goal of this project is to be able to autonomously control a K-9, rather than just remotely controlling the K-9. The current, remote-control set-up

requires that the handler be able to see the dog's position and heading. So, in order to mimic having a handler, accurate position and orientation need to be determined. After optimal position and orientation tracking has been achieved, a control algorithm will be used to autonomously control the K-9.

Figure 1 illustrates the "remote control" currently being used by the CDRI for the dogs.

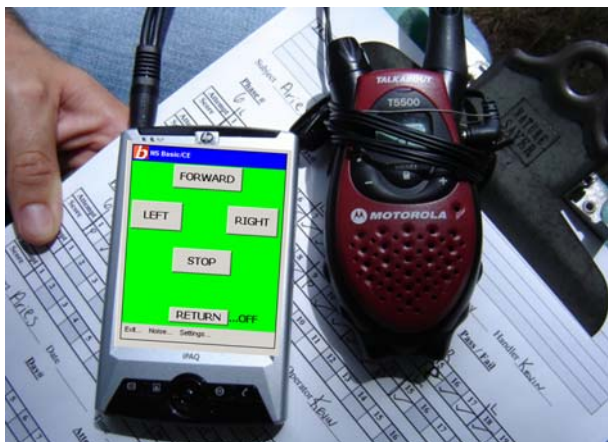


Figure 1: Canine remote control currently being used by the CDRI.

In order to map the location and orientation of the canine at a given point, a low-cost, limited sensor suite composed of a consumer grade uBlox GPS receiver and a six degree of freedom Sentera IMU containing three accelerometers and three gyroscopes was used. In this paper, only the accelerometer measuring acceleration in the longitudinal direction and the gyroscope measuring yaw rate were used. By combining the measurements from the GPS receiver, accelerometers, and gyroscopes using the Extended Kalman Filter (EKF), accurate estimates of the dog's position, orientation, and velocity can be provided to the dog's operator, or even a control system. A harness was designed for the canine that would hold the sensor suite as well as the vibrators and intercom system for instructing the canine motion.

Figure 2 illustrates the K-9, harness, and sensor suite utilized for the testing. The vibrators and intercom used for remote control purposes are not attached to the harness for the purposes of these tests. A new harness set-up is already being designed to make the sensor suite less bulky and heavy on the back of the canine. This will help to eliminate problems occurring due to the sensor suite sliding relative to the canine motion or producing extra noise on the measurements due to excessive shaking.



Figure 2: Canine with vest and GPS/INS system attached.

CANINE TESTING

Although the sensor suite currently being utilized to track the motion of the K-9 is not unique, the canine motion provided new challenges to motion tracking. For example, unlike what is typical when analyzing a vehicle, a canine bounces while trotting and also tends to slightly tilt back and forth while walking. Also, unlike man-made machines that respond in relatively predictable ways, the canine exhibits behaviors that are independent of the inputs. Therefore, many different possible canine motion situations must be accounted for in the design and tuning of the EKF algorithms. To account for these different scenarios, a series of controlled tests were run to demonstrate and determine the unique motion of a canine and to estimate the factors that could corrupt the navigation system.

Using a compass, estimated north and east axes were marked before applicable tests to provide qualitative measures of how effective the EKF was in tracking the canine position (see Figure 3). Next, the dog was walked to illustrate typical canine motions. Namely, the K-9 was instructed to:

- 1) Walk north; turn east; u-turn and walk west; then walk south ("L" test).
- 2) Walk east; turn and walk north, turn and walk west, then turn and walk south (box test).

Using these tests, the EKF was tuned to reject some of the typical disturbances created by a dog's sporadic movements, but still maintain an acceptable level of navigational performance. Videos were also made to assist in checking for error.

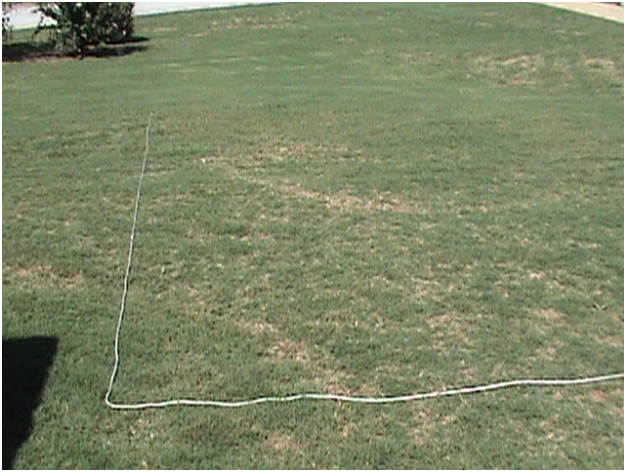


Figure 3: North and East axes.

TRACKING ALGORITHM

The Kalman Filter is an effective tool that can be used to integrate acquired measurements from a GPS sensor with acquired measurements from an Inertial Measurement Unit (IMU). Although GPS measurements prove to be relatively accurate, the rate at which they are taken is much slower than the rate at which an IMU takes measurements. Also, the GPS signal can be lost from time to time, but an IMU will be able to continue providing measurements. So, integrating the measurements from the different sensors can help to achieve more accurate results.

The EKF allows filtering of non-linear systems, such as those found in typical navigation filtering scenarios, and is described in detail elsewhere [1]. For this system, the longitudinal acceleration is measured by an accelerometer, and the yaw rate is measured by a gyroscope. The velocity, course, north, and east positions are measured by the GPS receiver. These are all integrated by the tracking algorithm. The state estimate vector for this system is:

$$\hat{x} = [\hat{V} \quad \hat{b}_a \quad \hat{\psi} \quad \hat{b}_g \quad \hat{N} \quad \hat{E}]^T \quad (1)$$

Where:

- \hat{V} = Estimated velocity
- \hat{b}_a = Estimated accelerometer bias
- $\hat{\psi}$ = Estimated course
- \hat{b}_g = Estimated gyroscope bias
- \hat{N} = Estimated north position
- \hat{E} = Estimated east position

Figure 4 visually illustrates the notations used in determining northern and eastern velocities.

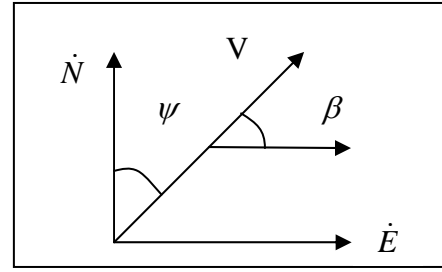


Figure 4: Visual illustration of northern and eastern velocity determination.

The GPS receiver outputs course ($\psi + \beta$). However, the gyroscope outputs yaw rate where the integral of yaw rate is heading. In order to integrate the yaw rate measurements with the GPS course measurements, the side slip, β , is assumed to be zero. Therefore, the estimated course ($\psi + \beta$) becomes estimated heading (ψ). The K-9 can induce errors into the EKF by not walking exactly forward when it is facing forward (i.e., the K-9 motion contains some sideslip). However, for the initial development of the tracking algorithm, this variable is neglected.

The state equations used for GPS/INS integration are as follows:

$$\hat{V} = A_x^m - b_a \quad (2)$$

Where: A_x^m = Measured longitudinal acceleration from the accelerometer

$$\hat{\psi} = g_z^m - b_g \quad (3)$$

Where: g_z^m = Measured yaw rate from the gyroscope measuring motion about the z-axis

The biases for this system are modeled as random walks, and the process noise is assumed to be zero mean white noise (i.e., $\omega \sim N(0, \sigma_\omega^2)$). Therefore, the following equations representing the change in biases for the accelerometer and gyroscope, respectively, are:

$$\dot{b}_a = 0 + \omega_a \frac{m}{s^2} \quad (4)$$

$$\dot{b}_g = 0 + \omega_g \frac{rad}{s}$$

Where: ω = Process noise

The estimated changes in northern and eastern directions are calculated with the following equations, according to Figure 4.

$$\begin{aligned}\hat{N} &= \hat{V} \cos \hat{\psi} \\ \hat{E} &= \hat{V} \sin \hat{\psi}\end{aligned}\quad (5)$$

Note that the northern and eastern velocities are non-linear. Therefore, the Jacobian (Φ) is used for the covariance prediction in the EKF to linearize the system about the operating point. The Jacobian is found utilizing the following:

$$\Phi = \begin{bmatrix} \frac{\partial f_1}{\partial x_1} & \dots & \frac{\partial f_1}{\partial x_n} \\ \vdots & & \vdots \\ \frac{\partial f_n}{\partial x_1} & \dots & \frac{\partial f_n}{\partial x_n} \end{bmatrix}\quad (6)$$

Where: $f_{1\dots n}$ = State equations
 $x_{1\dots n}$ = States

This results in the Jacobian matrix for the present system, shown below:

$$\Phi = \begin{bmatrix} 0 & -1 & 0 & 0 & 0 & 0 \\ 0 & 0 & 0 & 0 & 0 & 0 \\ 0 & 0 & 0 & -1 & 0 & 0 \\ 0 & 0 & 0 & 0 & 0 & 0 \\ \cos \hat{\psi} & 0 & -\hat{V} \sin \hat{\psi} & 0 & 0 & 0 \\ \sin \hat{\psi} & 0 & \hat{V} \cos \hat{\psi} & 0 & 0 & 0 \end{bmatrix}\quad (7)$$

There are two INS inputs to the integrated system—namely, A_x^m and g_z^m . Therefore, the input vector is the following:

$$u = \begin{bmatrix} A_x^m \\ g_z^m \end{bmatrix}\quad (8)$$

The above relationships and matrices are transferred into state space form. The general state space equation is the following:

$$\dot{x} = \Phi x + Bu + B_\omega \omega\quad (9)$$

Where: B = Input observation matrix
 B_ω = Noise input observation matrix

The general output or measurement equation is the following:

$$y = Cx + v\quad (10)$$

Where: v = Sensor noise
 C = Output observation matrix

The measured GPS velocity, V_{GPSM} , is equal to the actual velocity (state number 1) plus GPS sensor noise and similarly for the other GPS measurements. So, the output equation can be reduced to the following:

$$y = \begin{bmatrix} V_{GPSM} \\ \psi_{GPSM} \\ N_{GPSM} \\ E_{GPSM} \end{bmatrix}\quad (11)$$

The GPS Sensor Noise Covariance Matrix (R) and the Process Noise Covariance Matrix (Q) constitute the primary EKF tuning parameters.

$$R = \begin{bmatrix} \sigma_{GPSvel}^2 & 0 & 0 & 0 \\ 0 & \sigma_{GPShead}^2 & 0 & 0 \\ 0 & 0 & \sigma_{GPSnorth}^2 & 0 \\ 0 & 0 & 0 & \sigma_{GPSseast}^2 \end{bmatrix}\quad (12)$$

$$Q_k = \begin{bmatrix} \sigma_A^2 & 0 & 0 & 0 & 0 & 0 \\ 0 & \sigma_{bA}^2 & 0 & 0 & 0 & 0 \\ 0 & 0 & \sigma_g^2 & 0 & 0 & 0 \\ 0 & 0 & 0 & \sigma_{bg}^2 & 0 & 0 \\ 0 & 0 & 0 & 0 & \sigma_{north}^2 & 0 \\ 0 & 0 & 0 & 0 & 0 & \sigma_{east}^2 \end{bmatrix}\quad (13)$$

The Sensor Noise Covariance Matrix values are relatively standard and are acquired from the GPS sensor information.

$$\sigma_{GPSvel} = 0.05 \frac{m}{s}\quad (14)$$

$$\sigma_{GPSnorth} = 1.75 m$$

$$\sigma_{GPSseast} = 1.75 m$$

$$\sigma_{GPShead} = \frac{0.5}{V_{GPSM}} \text{ radians}$$

The Process Noise Covariance Matrix values prove to be more variable” due to the unique motion characteristics of a K-9.

$$0.01 \leq \sigma_A \leq 0.3 \frac{m}{s^2}\quad (15)$$

$$0.009 \leq \sigma_g \leq 0.02 \frac{rad}{s}$$

$$\sigma_{bA} \left(\frac{m}{s^2} \right) = \sigma_{bg} \left(\frac{rad}{s} \right) = 1 * e^{-10}$$

$$\sigma_{north} = \sigma_{east} = 1 * e^{-5} \text{ m}$$

Note that the optimal values for noise on the accelerometer and the gyroscope fall in a range of numbers based upon the particular test that the dog was instructed to run, rather than a unique value. It will be important to optimize the navigation algorithm to allow for unique values for a K-9 rather than for a particular path in the future. The process noise values also affect the dead reckoning performance of the system. So, further research must be conducted to optimize the performance of the navigation filter.

The state estimation covariance matrix was initialized as follows:

$$P = \begin{bmatrix} \sigma_{GPSvel}^2 & 0 & 0 & 0 & 0 & 0 \\ 0 & 1 & 0 & 0 & 0 & 0 \\ 0 & 0 & 1 * e^6 & 0 & 0 & 0 \\ 0 & 0 & 0 & 2 & 0 & 0 \\ 0 & 0 & 0 & 0 & \sigma_{GPSnorth}^2 & 0 \\ 0 & 0 & 0 & 0 & 0 & \sigma_{GPSeast}^2 \end{bmatrix} \quad (16)$$

The EKF is composed of a measurement update and a time update [1,18]. When GPS measurements are available, the following standard measurement update equations are applied.

$$L_k = P_k^- C_d^T [C_d P_k^- C_d^T + R_k]^{-1} \quad (17)$$

$$\hat{x}_k^+ = \hat{x}_k^- + L_k (y_k - C_d \hat{x}_k^-) \quad (18)$$

$$P_k^+ = (I - L_k C_d) P_k^- \quad (19)$$

Where: k = Current time index
 d = System is discretized
 L = Kalman gain vector

The EKF time update is described by:

$$P_{k+1}^- = \Phi_d P_k^+ \Phi_d^T + Q_k \quad (20)$$

$$\hat{x}_{k+1}^- = \hat{x}_k^+ + \dot{x}_{k+1} \Delta t \quad (21)$$

Where: \dot{x} is calculated from non-linear Equations (2-5).

As noted earlier, GPS outages can occur from time to time, particularly when objects come in between the GPS antenna and the satellites the receiver is tracking. Therefore, when the K-9 is instructed to maneuver into locations with more overhead obstacles, GPS could become unavailable. This initiates a dead reckoning situation, where only the IMU measurements are used in the filter. The accuracy in tracking the K-9 degrades over time since the tracking results are based solely on dead reckoning. Dead reckoning is less accurate, but integrating the IMU without GPS measurements still

provides positioning estimates, although at lower accuracy.

EXPERIMENTAL RESULTS

Figures 5 and 6 illustrate the challenge in attaining accurate tracking information when trying to utilize GPS/INS integration to accurately track K-9 motion. The figures show very high frequency and magnitude oscillations due to the motions of the K-9 (i.e., 100 deg/s oscillations for the yaw rate and three m/s² for the acceleration). Recall that one of the critical estimated states of interest for this study is the change in orientation of the K-9. However, much of this high frequency motion is due to the unique motion characteristics of the K-9, rather than the actual orientation change of the K-9. The motions of the dog captured by the yaw gyroscope, for instance, are at a relatively higher frequency than the actual change of in the dog's orientation. This illustrates the need for further optimizing of the filtering in future work.

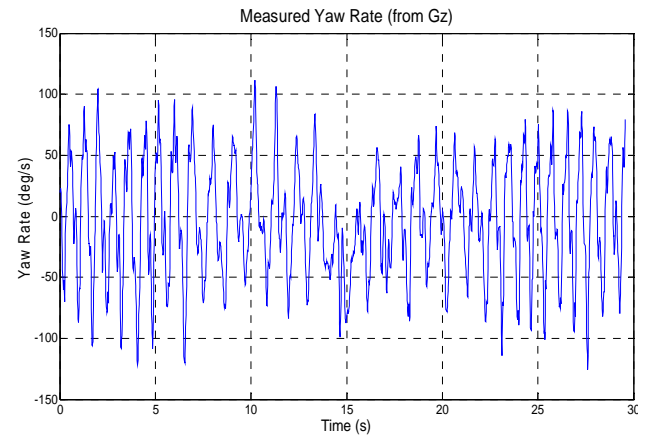


Figure 5: Yaw rate measured from the IMU gyroscope.

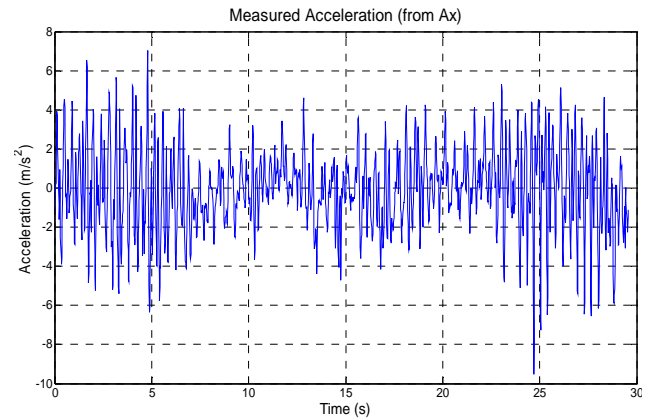


Figure 6: Measured acceleration from the longitudinal accelerometer.

Figures 7, 8, and 10 illustrate the results acquired when the K-9 is instructed to travel north, turn and travel east, U-turn and travel west, and then turn and travel south. Figure 7 illustrates measured GPS velocity, EKF estimated velocity, and the velocity acquired from pure dead reckoning of the IMU without sensor biases taken into account. Again, the EKF estimate tracks the dog very well. The dead reckoning velocity profile drifts away from the GPS measurement and EKF estimate, as would be expected.

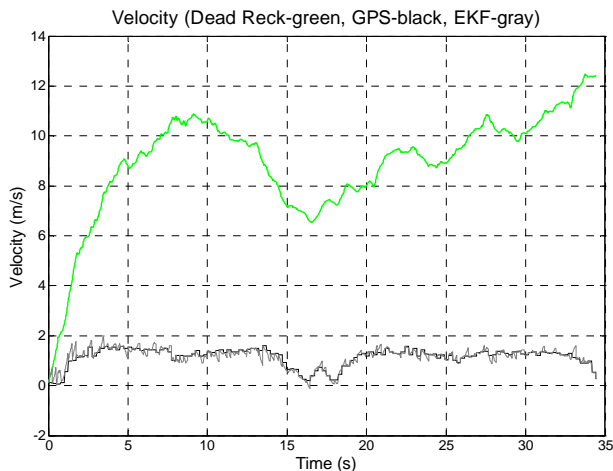


Figure 7: Velocity profile for GPS measurements versus EKF estimate versus dead reckoning when the K-9 travels north, turns and travels east, U-turns and travels west, and then turns and travels south.

The EKF position estimate (see Figure 8) adheres to the GPS measurements, then diverges when the dog velocity approaches zero meters per second at the U-turn around 16 and 18 seconds, which caused the GPS course measurements to become inaccurate. Then, when the K-9 velocity increased, the positions merge again towards the end of the test.

Additionally, as seen in Figure 10, the biases level out over time, and the velocity and heading track the GPS very well. The heading drifts slightly when the K-9 velocity approaches zero meters per second at the U-turn (see Figure 10).

Figures 9 and 11 illustrate the results acquired when the dog is instructed to travel north, turn and travel east, turn and travel south, and then turn and travel west to the approximate starting position. GPS is artificially removed around 15 seconds to demonstrate loss of GPS and simulate pure dead reckoning. The EKF estimate at this point is based on the IMU and the last bias estimate before GPS cut out alone for about 15 seconds. The EKF estimate velocity profile shows the commencement of a severe drift away from the actual GPS measurements towards the end of the test (see Figure 11). The biases become constant after GPS cuts out. Although the

velocity drifts, the heading estimate continues to stay close to the actual GPS measurements.

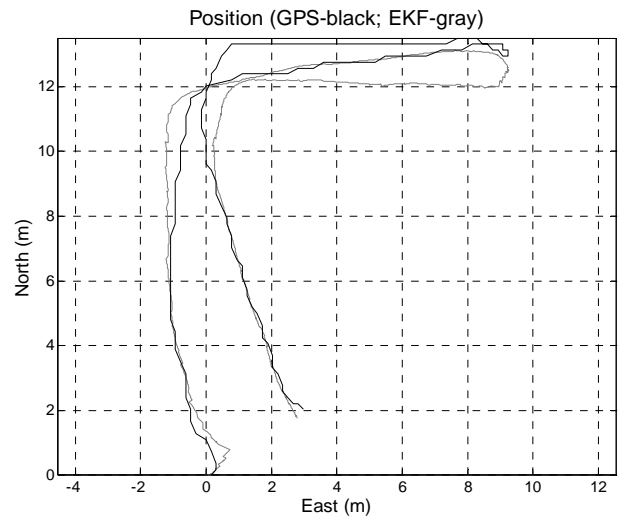


Figure 8: GPS measurement versus EKF estimated position results when the K-9 travels north, turns and travels east, U-turns and travels west, and then turns and travels south.

The position plot (Figure 9) shows the measured GPS position and EKF estimated position of the K-9 during the test. The EKF estimate drifts away from the GPS measurements towards the end of the test, as would be expected due to the simulation of GPS outage half-way through the process.

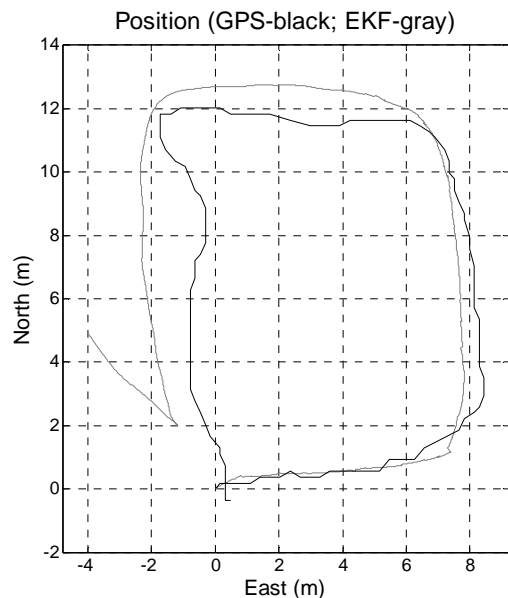


Figure 9: GPS measurement versus EKF estimated position results when the K-9 travels north, turns and travels east, turns and travels south, and then turns and travels west. GPS measurements are turned off in the EKF estimate at approximately 15 seconds.

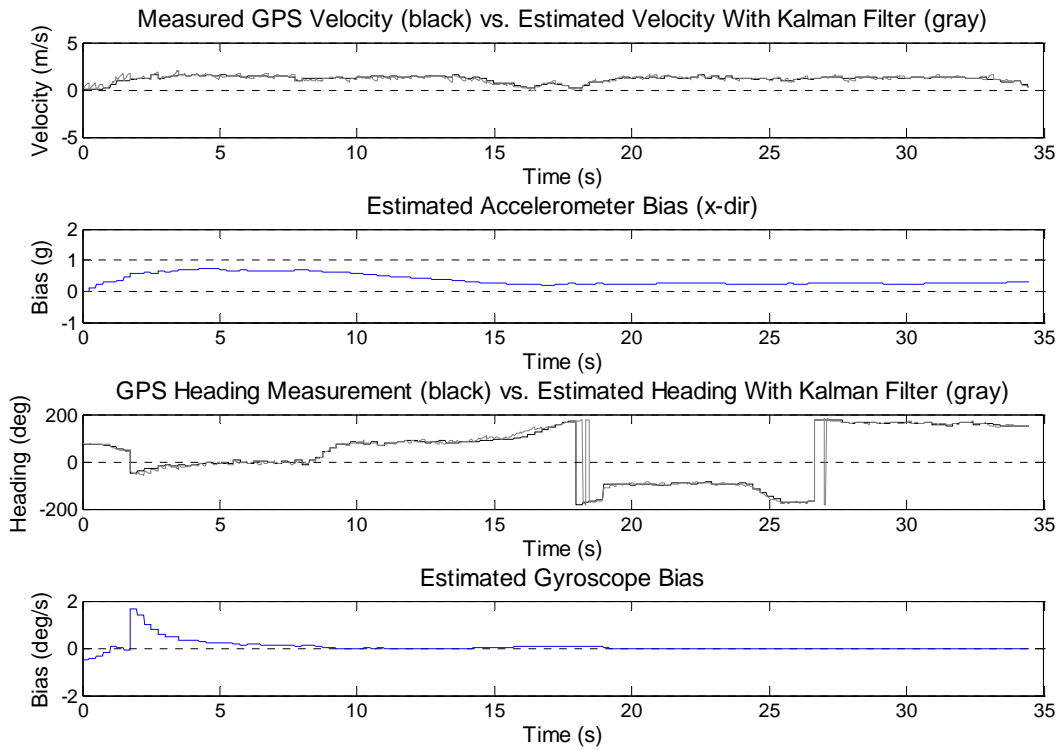


Figure 10: Velocity, accelerometer bias, heading, and gyroscope bias EKF estimate results when the K-9 travels north, turns and travels east, U-turns and travels west, and then turns and travels south.

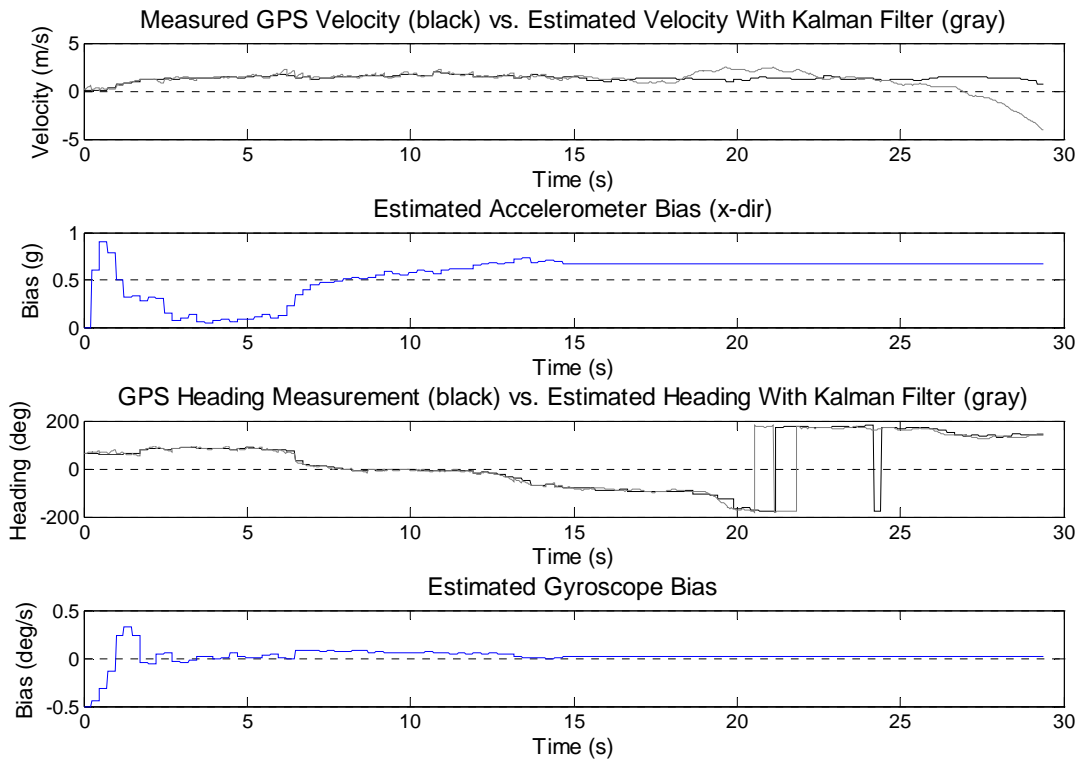


Figure 11: Velocity, accelerometer bias, heading, and gyroscope bias EKF estimate results when the K-9 travels north, turns and travels east, turns and travels south, and then turns and travels west. GPS measurements are turned off in the EKF estimate at approximately 15 seconds.

CONCLUSIONS

This paper has shown that GPS/INS integration can be utilized effectively to achieve adequate position and orientation results with the Extended Kalman Filter, in spite of the unique motion characteristics of the K-9. However, future work must optimize the above navigation algorithm to more efficiently track the dog's motion characteristics in light of Figures 5 and 6. Also, in this paper the process noise parameters had to be tuned for each experiment or path. It is desired that the process noise parameters be path independent. So, without having to make adjustments to the values of the process noises, the tracking algorithm must be robust enough to handle erratic disturbances such as the following:

- 1) The canine jumps;
- 2) The canine bends over to sniff, as bomb and drug detection canines do;
- 3) The canine runs, thus causing the sensor suite to slide on the back of the dog.

Also, in actuality, the assumption that the process noise is zero mean and white is incorrect. The noise may need to be modeled differently to achieve better results. It is also possible that sideslip cannot be neglected. Although a vehicle has little side slip in typical situations, a dog may tend to slide a bit while walking forward, which would imply that the GPS course measurements do not reduce to heading.

On the hardware side, the sensor suite components will probably be separated and embedded into the dog's harness in the near future rather than being placed in a bulky and heavy box on the dog's back that tends to slide around on the K-9. It is also possible that a simple, digital magnetic compass could be utilized in this application to help improve heading performance, as well as including measurements from some of the other IMU components.

ACKNOWLEDGMENTS

Special thanks to Kevin Mullins and Auburn University's Canine & Detection Research Institute for their excellent work in training dogs to respond to remote control, and their continuing work in broadening the dog's abilities. Thanks also to Cory Steigerwald for the use of his dog for K-9 motion characteristic testing. This work was supported by the Office of Naval Research, Award # N00014-06-1-0518.

REFERENCES

- [1] R. Stengel. *Optimal Control and Estimation*. Dover Publications, Mineola, NY. 1994. ISBN: 0-486-68200-5.
- [2] D.M. Bevly. "Evaluation of a Blended Dead Reckoning and Carrier Phase Differential GPS System for Control of an Off-Road Vehicle," *Ion GPS '99*. Nashville, TN. 14-17 Sep., 1999. pp. 2061-2069.
- [3] S. Godha. "Performance Evaluation of Low Cost MEMS-Based IMU Integrated with GPS for Land Vehicle Navigation Application," MS Thesis, University of Calgary. Feb., 2006.
- [4] J. Ryu, J.C. Gerdes. "Integrating Inertial Sensors with GPS for Vehicle Control," *Jour. of Dynamic Systems Measurement, and Control*, vol. 126, Issue 2. June, 2004. pp. 243-254.
- [5] D.M. Bevly. "Global Positioning System (GPS): A Low-Cost Velocity Sensor for Correcting Inertial Sensor Errors on Ground Vehicles," *Jour. of Dynamic Systems Measurement, and Control*, vol. 126, Issue 2. June, 2004. pp. 255-264.
- [6] T.N. Upadhyay, S. Cotterhill, A.W. Deaton. "Autonomous GPS/INS Navigation Experiment for Space Transfer Vehicle," *IEEE Transactions on Aerospace and Electronic Systems*, vol. 29(3). Jul., 1993. pp. 772-785.
- [7] V. Gabaglio. "GPS/INS Integration for Pedestrian Navigation," PhD dissertation, Institute of Geomatics of the Swiss Federal Institute of Technology in Lausanne. 2003.
- [8] O. Ladetto, V. Gabaglio, B. Merminod. "Combining Gyroscopes, Magnetic Compass and GPS for Pedestrian Navigation," *Proc. Int. Symposium on Kinematic Systems in Geodesy, Geomatics and Navigation (KIS 2001)*. 2001. pp. 205-213.
- [9] A.J. Hill, A. Slamka, Y.T. Morton, M. Miller, J. Campbell. "A Real-Time Position, Velocity, and Physiological Monitoring and Tracking Device for Equestrian and Race Training," *Proceedings of the ION GNSS*. Sept. 2007.
- [10] W.J. Gomes, III, D. Perez, Jr., J.A. Catipovic. "Autonomous Shark Tag with Neural Reading and Stimulation Capability for Open-ocean Experiments," *Eos Trans. AGU*. 87(36), Ocean Sci. Meet. Suppl., Abstract OS45Q-05. 2006.
- [11] Shandong University of Science and Technology. "SDUST Created Remote-controlled Pigeon," 2 Sep., 2007. http://www.sdkd.net.cn/en/news_show.php?id=65. 12 Sep., 2007.
- [12] S. Brown. "Stealth sharks to patrol the high seas," *New Scientist*. 4 Mar., 2006. pp. 30-31.
- [13] Y. Li, S. Panwar. "A Wireless Biosensor Network Using Autonomously Controlled Animals," *IEEE Network*, May/June, 2006. pp. 6-11.
- [14] S. Talwar, S. Xu, E. Hawley, S. Weiss, K. Moxon, J. Chapin. "Rat navigation guided by remote control," *Nature*, vol. 417(6884). May, 2002. pp. 37-38.
- [15] Holzer R, Shimoyama I, Miura H. "Locomotion Control of a Bio-Robotic System via Electric Stimulation," International Conference on Intelligent Robots and Systems. Grenoble, France. 1997.

- [16] W. Song, J. Chai, T. Han, K. Yuan. "A Remote Controlled Multimode Micro-stimulator for Freely Moving Animals," *Acta Physiologica Sinica*, 58(2). 25 Apr., 2006. pp. 183-188.
- [17] VNUnet UK. "Researchers Develop 'Robo-roach,'" UNU-MERIT: I&T Weekly, Iss. 7. 28 Sep., 2001. United Nations University. 13 Sep., 2007. http://www.merit.unu.edu/i&tweekly/i&tweekly_previous.php?issue=0107&issue_show=7&year=2001.
- [18] G. Franklin, D. Powell, M. Workman. *Digital Control of Dynamic Systems*, 3rd Edition, Addison Wesley Longman Inc., Menlo Park, CA. 1998.